Proceedings of ERAD (2004): 281–285 © Copernicus GmbH 2004

ERAD 2004

Deriving turbulent kinetic energy dissipation rate within clouds using ground based radar

D. Bouniol[1], **A. Illingworth**[2], **and R. Hogan**[2]

[1]Centre d'Etude des environnements Terrestre et Planétaires, CNRS, Vélizy, France
[2]Department of Meteorology, University of Reading, Reading, UK

1 Introduction

Small-scale turbulence has an important influence on the cloud structure and therefore on the spatial distribution of the optical and microphysics properties. Turbulence is also directly linked to the life cycle of the clouds through internal mixing and entrainment processes. A good way to estimate the turbulence activity is to measure the turbulent kinetic energy (TKE) dissipation rate (ϵ) which represents the rate of conversion of TKE into heat or in other words the rate at which the TKE is dissipated by viscosity.

Several methods have been proposed in order to derive this parameter from observations. The most common one is to perform spectral analysis on aircraft data (for instance Gultepe and Starr, 1995; Smith and Del Genio, 2001) or from ground based radar data (Brewster and Zrnić, 1986). Another technique is to derive ϵ from ground based spectral width measurements such as Chapman and Browning (2001) or Kollias et al. (2001). Turbulence inferences made at vertical incidence such as those by Kollias et al. (2001) may be biased, especially at low turbulence levels, because of the contribution from the spread of terminal velocities in the particle size distribution.

In this paper a new method, inspired by the early work of Rogers and Tripp (1964), is presented. It consists in exploiting the very high temporal resolution of Doppler measurements performed by ground based 94 GHz radar in order to derive ϵ within non-precipitating clouds which can be composed of water droplets such as stratocumulus or ice crystals such as cirrus.

As a first step the principle of the method is explained, the sensitivity of the estimate is then tested against several parameters, finally the method is applied to data collected by the 94 GHz radar of Chilbolton (UK) operated in the framework of European Project CloudNet.

Correspondence to: D. Bouniol
(dominique.bouniol@cetp.ipsl.fr)

2 Principle

First of all it must be assumed that the radar targets (e.g. water droplets or ice crystals) are good tracers of the turbulent motions; this is why this method is only applied to non-precipitating ice clouds or to particular water clouds such as stratocumulus which contain only small drizzle droplets. Indeed a particle with low inertia is more able to follow turbulent motions than a particle with a high inertia. As a second step the TKE spectrum is assumed to be Kolmogorov in form which means that turbulence is isotropic and homogeneous at the scale sampled by the radar.

Figure 1 displays the shape of the TKE spectrum and shows that within the inertial subrange a relationship should exist between the large-scale velocity fluctuations and the TKE dissipation which occurs at wavelengths of a centimeter or less.

Kolmogorov's theory states that, within the inertial subrange, the spectral density can be expressed as:

$$S(k) = a\epsilon^{2/3}k^{-5/3} \tag{1}$$

where a is the universal Kolmogorov constant with a value of 1.62 and k is the wave number.

Rogers and Tripp (1964) show that the average TKE per unit mass of air (E) can be written as:

$$\sigma_{\overline{v}}{}^2 + \overline{\sigma_t{}^2} = 2E \tag{2}$$

where $\sigma_{\overline{v}}{}^2$ is the variance of the mean Doppler velocity and $\sigma_t{}^2$ is the variance due to turbulence within the pulse volume. In addition to having the property that their sum is proportional to the TKE the two variances are such that their relative magnitudes indicate the manner in which the TKE is partitioned between different scales. The variance $\sigma_{\overline{v}}{}^2$ of the mean wind is an indicator of the kinetic energy in turbulent scales that are generally larger than the dimensions of the sampled volume. Conversely the average variance $\overline{\sigma_t{}^2}$ is an indicator of the kinetic energy energy in the small scales of turbulence (Rogers and Tripp, 1964).

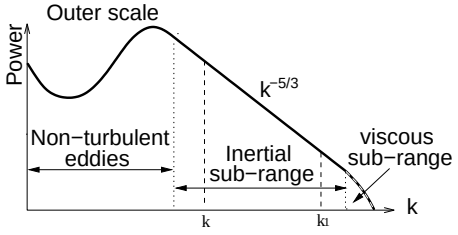

Fig. 1. Schematic plot of the TKE spectrum. The dotted line indicates the different regions of the TKE spectrum which are labelled. The dashed line corresponds to integration limits (see text for explanation)

These variances can be thought of as part of the TKE spectrum. The variance due to turbulence within the pulse volume may be rewritten as follows:

$$\sigma_t{}^2 = \int_{k_1}^{k_2} a\epsilon^{2/3}k^{-5/3}dk \tag{3}$$

where $k_2 = 2\pi/L_2 = \lambda/2$ is the smallest scale that can be probed by the Doppler radar, ultimately $\lambda/2$ (where λ is the radar wavelength), $k_1 = 2\pi/L_1$ is related to the scattering volume dimension and so includes large eddies traveling through the sampling volume during the dwell time (Kollias et al., 2001). This variance contributes directly to the spectral width and must be extracted from the other contributions to spectral width, such as wind shear and particle terminal fall speed, if we want to estimate ϵ from this measurement (see for instance Chapman and Browning, 2001; Kollias et al., 2001).

In the same way the variance of the mean Doppler from successive spectra can also be expressed:

$$\sigma_{\overline{v}}{}^2 = \int_{k}^{k_1} a\epsilon^{2/3}k^{-5/3}dk \tag{4}$$

where $k = 2\pi/L$ is related to the large eddies travelling through the sampling volume during the sampling time (typically about 30 s). The different L parameters represent the length scales related to each wave number.

By integrating this last expression ϵ leads to:

$$\epsilon = \left(\frac{2}{3a}\right)^{3/2} \frac{\sigma_{\overline{v}}{}^3}{\left(k^{-2/3} - {k_1}^{-2/3}\right)^{3/2}} \tag{5}$$

The main contribution to k is due to the advection of clouds by the wind through the beam, a distance which is generally much larger than the width of the radar beam at a given altitude. In this paper the horizontal wind is derived from the ECMWF analysis (stored every hour at the same geographical location in the framework of the CloudNet project). The wave number can be computed as:

$$k = \frac{2\pi}{L} = \frac{2\pi}{x_b + T_s\|\overrightarrow{V_h}\|} \tag{6}$$

where T_s is the sampling time, $\|\overrightarrow{V_h}\|$ the modulus of the horizontal wind interpolated from the hourly analysis and x_b is the width of the radar beam at a height z. This width can be computed by using $x_b = 2z\sin(\theta/2)$ with θ=0.5°, the beamwidth, in the case of the Chilbolton 94 GHz radar.

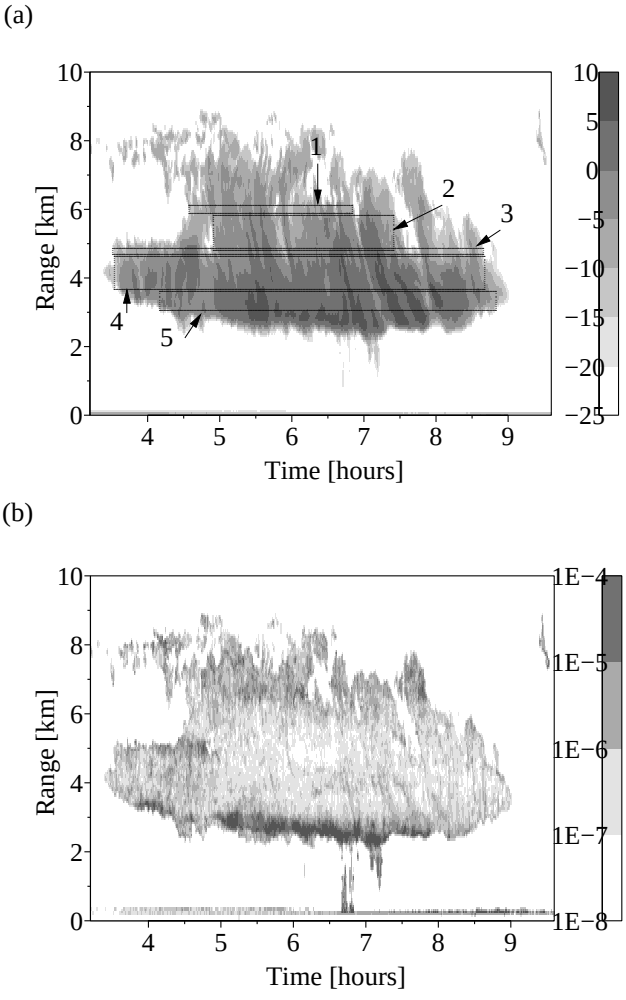

Fig. 2. (a) Reflectivity in [dBZ] observed by the vertically pointing 94 GHz Doppler radar at Chilbolton (UK) on the 17 July 2001. (b) Estimated ϵ in [m^2s^{-3}] by using the previous explained method. The boxes displayed within the cloud and labelled from 1 to 5 are used for validation in the next section.

As an illustration the method is applied to a deep ice cloud observed on the 17 July 2001 within a pre-frontal system. Figure 2a shows the observed reflectivity which is in the range −25 dBZ to 10 dBZ. Lower values than −25 dBZ are not detected at this time due to a loss of sensitivity of the radar at this time (see Hogan et al., 2003). Figure 2b shows the values of ϵ which range from 10^{-4} m^2 s^{-3} at the base of the cloud to 10^{-8} m^2 s^{-3} within the cloud core. These values are in the same range as those obtained in previous studies (see for instance the summary table of Gultepe and Starr, 1995).

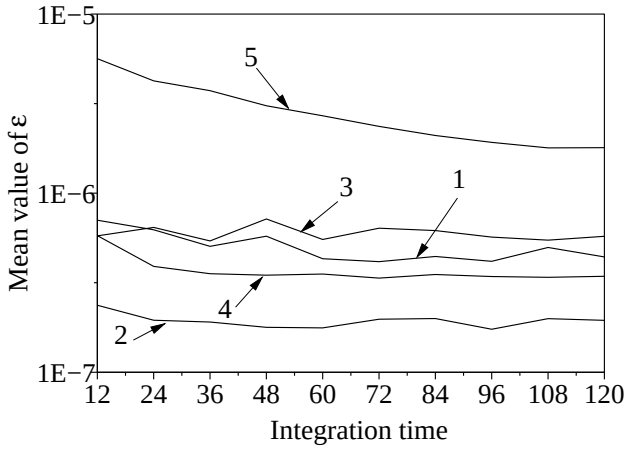

Fig. 3. Mean value of ϵ in [$m^2.s^{-3}$] for the areas shown on Fig. 2a computed for different integration times in [s].

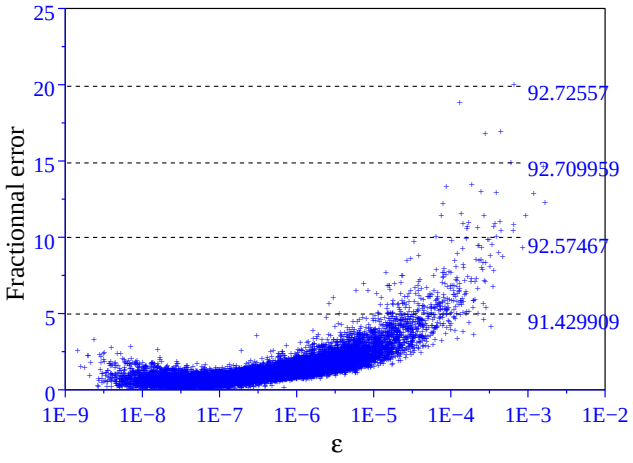

Fig. 4. Scatter plot of fractionnal error on $\sigma_{\overline{v}}$ in percentage as a function of estimated ϵ. The numbers on the right hand side give the cumulative amount, in percentage, of estimates lower than the value given on the Y-axis by the dashed line.

3 Sensitivity study

To evaluate the validity of this method one has to test the sensitivity to the different parameters introduced in the ϵ computation. It has been assumed that the TKE dissipation spectrum is Kolmogorov in form i.e. that it can be expressed as a $k^{-5/3}$. A good way to test this point is to compute $\sigma_{\overline{v}}$ for different integration times. As can be seen from Eq. (6) varying the integration time will change the value of k and hence the integrated part of the spectrum (see Fig. 1).

To test this hypothesis ϵ has been computed for different integration times. Since changing the integration time modifies the resolution of time series a point to point comparison is impossible. Mean values of ϵ are then computed in the different boxes displayed in Fig. 2a. The results of mean for each box as a function of the integration time are displayed in Fig. 3.

It can be observed that the mean value of ϵ for a given box is almost constant once the integration time is larger than 24 s. For the box 5 the value of ϵ seems to be more variable. A slight variation in the results is systematically observed for the 12 and 24 s dwells, this can caused by k_1 falling within the viscous sub-range (see Fig. 1) and k very close to this value. In this configuration the integrated part of the spectrum is far from a $k^{-5/3}$ law.

The influence of terminal fall velocity in $\sigma_{\overline{v}}$ has also to be quatified. Indeed the mean Doppler velocity measured by a vertically pointing radar is the result of the contribution of vertical air velocity w and of terminal fall velocity of hydrometeor Vt. If one want to derive ϵ from $\sigma_{\overline{v}}$ one has to show that the main contribution is from the variance of the w, the variance of V_t being related to variations in the microphysics within the volume sampled by the radar in 30 s.

When no (or low) attenuation exists, which is the case within ice clouds, V_t can be derived from the reflectivity by using statical relationships of the form $V_t = aZ^b$ **?** or **?**. In case of deep ice clouds the couple of values (a, b) is varying (0.8, 0.25) to (1, 0.5).

An error analysis can also be performed on the estimate of ϵ. A simple error calculation leads to the following expression:

$$\frac{\Delta\epsilon}{\epsilon} = 3\frac{\Delta\sigma_{\overline{v}}}{\sigma_{\overline{v}}} + \frac{T{k_1}^{1/3} - T_s k^{1/3}}{k^{-2/3} - {k_1}^{-2/3}} \frac{\Delta\|\overrightarrow{V_h}\|}{2\pi} \tag{7}$$

where T is the sampling time associated to k_1.

This equation shows that the fractional error on ϵ is three times the fractionnal error on $\sigma_{\overline{v}}$. The error on $\sigma_{\overline{v}}$ can be estimated assuming that $\sigma_{\overline{v}}$ is a randomly distributed variable. In this case this variable is completely characterised by its first and second moment. Following Saporta (1990) the second moment of a variance estimator can be written:

$$\sigma_{\sigma_{\overline{v}}} = \sqrt{\frac{N-1}{N}\left[(N-1)\mu_4 - (N-3){\sigma_{\overline{v}}}^4\right]} \tag{8}$$

where N is as before the sample number used for estimation and μ_4 is the fourth moment of the sample. This second moment can be identified to the accuracy of an estimator.

This fractionnal error on $\sigma_{\overline{v}}$ has been computed for a prefrontal cloud observed on the 27 November 2001 (the result being similar for other cases) and is displayed on Fig. 4 as a function of ϵ. The number on the right hand side of the figure shows the cumulative amount of values lower than the value shown by the dashed line. For instance it can be observed that more that more than 91% of the data have a fractional error lower than 5% which leads to a fractional error on ϵ lower than 15% which is an acceptable value if it is compared to the accuracy obtained by other methods.

The fractionnal error of the horizontal wind can be quantified (not shown here) and is still lower than 0.15. If the wind is assumed to be known better than 0.5 $m\,s^{-1}$, it leads to a fractionnal error on ϵ of about 7.5%. Summing the two error contributions leads to a fractionnal error of 22.5% for more than 90% of the points.

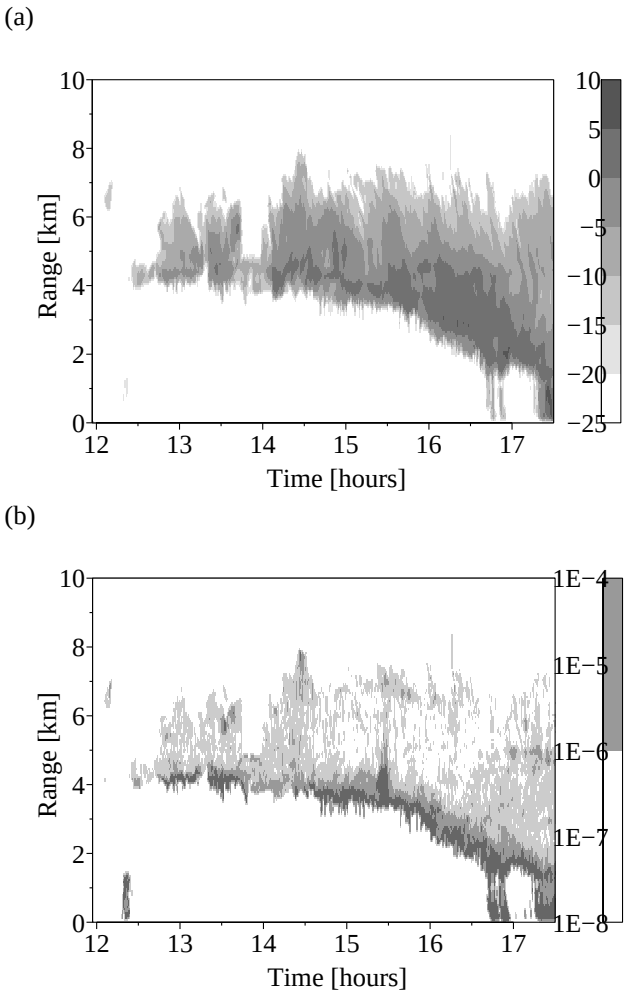

Fig. 5. (a) Reflectivity in [dBZ] observed by the vertically pointing 94 GHz Doppler radar at Chilbolton (UK) on the 18 January 2002. (b) ϵ in [m^2 s^{-3}] method.

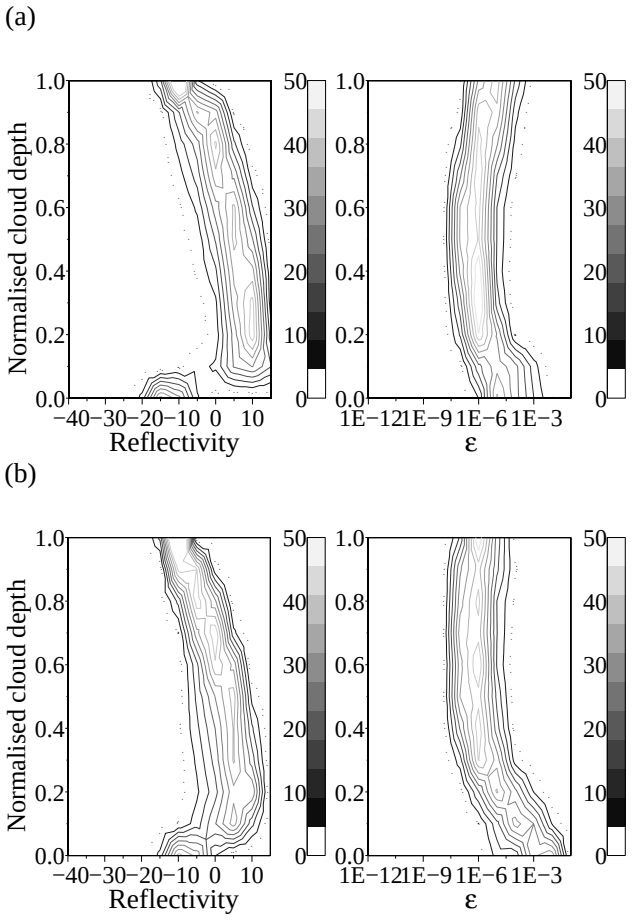

Fig. 6. Normalised histograms of reflectivity in [dBZ] (left plot) and ϵ in [m^2 s^{-3}] (right plot) as a function of normalised cloud depth. (a) For the 17 july 2001 and (b) for the 18 january 2002. The color scale gives the representativity of a given value for a given level in percentage.

4 Results

One of the main strengths of this approach is that ϵ can be evaluated for a large data set of radar measurements, provided that the time resolution is such that the data are within the inertial sub-range and that an estimate of the horizontal wind is available. It is then possible to investigate if some common characteristics exist for the dissipation of TKE within different kind of clouds and to see if these characteristics are related to the microphysical, radiative and dynamical processes within the clouds.

Previous work Chapman and Browning (2001) has demonstrated that turbulence activity can balance the tendency of fronts to collapse under frontogenesis. They conclude that with the increase of model resolution, it may become necessary to represent turbulent activity at all levels within model. This representation can only be performed if systematic behaviour are derived. This method has been applied to the CloudNET data set, where three cloud radars are continuously operated at vertical incidence. The data used in this paper are collected at the Chilbolton observatory in UK and following the work of Chapman and Browning (2001) application is restricted to frontal systems which are anounced by thin high level cirrus depening for several hours and leading to precipitations about 6 hours later.

Figure 5a shows the typical reflectivity pattern observed in such clouds, this case being observed on the 18 January 2002. On this figure the cloud deepening as the system approach the observatory is obvious. ϵ has been computed using the method presented in this paper. One can observe the same behaviour as on Fig. 2b with a strong increase of ϵ values near cloud base.

To make comparisons easier, histograms of various cases can be built up, however if one wants to compare cloud with different altitude and depth, one needs to normalise the altitude respectively to cloud depth. The cloud is divided in ten equally deep layers (the lowest being cloud base) and the reflectivity and ϵ values are taken at the middle of the layer, then for each level a normalised histogram is calculated. This way the behaviour of different level within clouds (for instance cloud base, cloud core and transition from one part to another) can easily be compared from one case to another.

Left part of Fig. 6 shows the normalised histograms of reflectivity for the two frontal case ((a) for the 17 july 2001 and (b) for the 18 january 2002). The lightest grey (10 in our case) gives the more propable value of reflectivity for each level as a function of cloud depth. In both cases it is then observed an increase larger than 20 dBZ at cloud base (passing from the first level to the second one) and a more transitory decrease of reflectivity (begining at aout level 6) of about 10 dBZ. The right part of Fig. 6 show an anti-correlated histogram: the turbulence activity decreases as the reflectivity increases. The decrease at cloud base is about two orders of magnitude as it is about one order of magnitude at cloud top. The large values of ϵ at cloud base can be explained by the evaporation of ice particles falling in an unsaturated environment, this evaporation relaxes latent heat which tends to increases the mixing process and then increase this evaporation. A process of the same kind can be suspected at cloud top, but instead of evaporation due to particle falling in this case it could be detrainment at cloud top. The two cases shown here are behaving in a very similar manner (even if in one case we have a summer front and in the second a winter front), and if the study is extended to the whole CloudNET data set one can observe exactly the same kind of profiles. At this point it would be interested to introduced such a turbulent dissipation of ice cloud particle in a mesoscale model in order to study in a more diagnostic way its influence on the cloud life.

5 Conclusions and persepectives

A new method to estimate the TKE dissipation rate ϵ within ice clouds or light-precipitating clouds using vertically pointing radar is proposed. The requirement is that the sampling resolution is sufficient to be sure the Kolmogorov theory applied and that an estimate of the horizontal wind is available. In this paper this estimate is comming from the operational model of the ECMWF, but for instance the estimation given rawinsondes can also be used.

A sensitivity analysis has been presented, showing that the accuracy of the method is about 20%. At this step a closer comparison with other method would be interesting, in particular with the one deriving ϵ from the spectral width.

This method has been applied to pre-frontal cloud cases present within the CloudNET data base and systematic behaviours can be derived : an increase of the turbulent activity at cloud base assumed to be related to evaporation of ice particles falling in a an unsaturated environment and at cloud top which can be related to entrainment. However further investigations are needed to determine how this process influences the cloud life.

Acknowledgements. This work was carried out with the support of EU CloudNet contract EVK2-CT-2000-00065 and NERC grant NER/T/S/1999/00105.

References

Brewster, K. A. and Zrnić, D. S.: Comparison of Eddy Dissipation Rates from Spatial Spectra of Doppler Velocities and Doppler Spectrum Widths, J. Atmos. Oceanic Technol, 3, 440–452, 1986.

Chapman, D. and Browning, K. A.: Measurements of dissipation rate in frontal zones, Quart. J. Roy. Meteor. Soc., 122, 1939–1960, 2001.

Kollias, P., Albrecht, B. A., Lhermitte, R. and Savtchenko, A.: Radar Observations of Updrafts, Downdrafts, and Turbulence in Fair-Weather Cumuli, J. Atmos. Sci., 58, 1750–1766, 2001.

Gultepe, I. and Starr, D. O'C.: Dynamical Structure and Turbulence in Cirrus Clouds: Aircraft Observations during FIRE, J. Atmos. Sci, 52, 4159–4182, 1995.

Hogan, R. J., Bouniol, D., Ladd, D. N., O'Connor, E. J., and Illingworth, A. J.: Absolute calibration of 94/95 GHz radars using rain, J. Atmos. Oceanic Technol., 20, 572–580, 2003.

Hogan, R. J. and Illingworth, A. J.: Parameterizing ice cloud inhomogeneity and the overlap of inhomogeneities using cloud radar data, J. Atmos. Sci., 60, 756–767, 2003.

Rogers, R. R. and Tripp, B. R.: Some Radar Measurements of Turbulence in Snow, J. Appl. Meteor., 3, 603–610, 1964.

Saporta, G.: Probabilités, analyse des données et statistiques. Ed. TECHNIP, 1990.

Smith, S. A. and Del Genio, A. D.: Analysis of Aircraft, Radiosonde, and Radar Observations in Cirrus Clouds Observed during FIRE II: The Interactions between Environmental Structure, Turbulence, and Cloud Microphysical Properties, J. Atmos. Sci., 58, 451–461,2001.